International Research Journal of Engineering and Technology (IRJET) e-ISSN: 2395-0056
Volume: 04 Issue: 12 | Dec-2017 www.irjet.net p-ISSN: 2395-0072

SERIES VOLTAGE COMPENSATOR MODELING AND DESIGN FOR REDUCTION OF GRID-TIE SOLAR INVERTER DC-LINK CAPACITANCE

AMMALLADINNE LALITHA[1], M.SUBRAMANYAM[2], M. SHOBBHA[3], B. NARENDRA[4]

ABSTRACT: A grid-tie solar inverter with an arrangement voltage compensator for diminishing the high-voltage dc-connect capacitance is exhibited. The compensator gets vitality from the dc connect to maintain the voltage on its dc side and generates an air conditioner voltage to balance the voltage ripple on the dc interface. As the compensator forms little ripple voltage on the dc connect and receptive power, it can be actualized with low-voltage devices, and thus, its voltamp rating is little. As the required vitality stockpiling of the dc interface, shaped by a lessened estimation of the dc-connect capacitor and the compensator, is decreased, the architecture permits supplanting prevalently utilized electrolytic capacitors with choices of longer lifetime, such as power film capacitors, or expanding the system lifetime regardless of whether there is a critical reduction in the capacitance of electrolytic capacitors because of maturing. Definite mathematical examination on the static and dynamic behaviors of the general system, and the control method will be introduced. A streamlined plan strategy for the compensator will be given. A 2-kW, 220-V, 50-Hz model has been assembled and assessed. The theoretical forecasts are contrasted positively and experimental results. At long last, the execution cost with electrolytic-capacitor and compensator for the dc connection will be thought about.

1. INTRODUCTION

In today's eco-conscious world, the rapid pace of advancement in smart grid technology has a positive effect on the electricity industry reforms. The goal is to use smarter control of distributed energy sources combined with intelligent demand side management to improve the overall efficiency and reliability of the power grid. Regardless of the type of the distributed power generation unit used, the electricity generated by the renewable energy source is processed through a power conditioning system that performs several functions. First, it fabricates an optimal power matching condition for the renewable energy source to deliver maximum power to the power conditioning system. Second, it manages energy flow among the renewable energy source, energy storage system, and surrounding ac and/or dc networks or systems. Third, it produces high-quality power to and from the energy storage system, loads, and connected grid. Finally, it is capable of providing tight output regulation and handling fast transient and dynamic response to external disturbances.

Typical power conditioning systems consist of multiple switching-mode power converters. In order to provide high degree of controllability and flexibility of power flow, the electrical energy generated by renewable energy source is converted into dc power while the one delivered to the other part of the system or load is converted from the dc power. Thus, power converters are all interconnected through a dc link. To ensure a stable operation of the power conditioning system, the dc-link voltage is stabilized by a capacitor bank, which is sometimes the dominant part in terms of the physical volume and cost. Among the different types of capacitors, aluminum electrolytic capacitors are a popular choice for the capacitor bank, due to their high capacitances in a small form factor. However, their life expectancy is comparatively short and is reduced dramatically with elevated ambient temperatures. Statistics reveals that up to 30% of electronic system failures are due to malfunctions of capacitors. Thus, capacitors are sometimes a reliability bottleneck. For high-voltage high-power conversion systems, dc-link capacitors are usually periodically replaced and monitored for reliable and safe operation. Leading to substantial maintenance costs and electronic waste production. To enhance reliability and lifetime, high-performance capacitors, like power film capacitors, have been used as replacements for some electrolytic capacitors.

II. OPERATION OF THE SERIES VOLTAGE COMPENSATOR

Fig. 1 shows the architecture of the grid-tie solar inverter system with a series voltage compensator connected to he dc link. The system consists of two power conversion stages. The front stage is a dc–dc boost converter. It is connected between a string of solar panels and the dc link. The output stage is a grid-tie dc–ac converter, which is connected between the dc link and the power grid. The compensator, which is a capacitor supported full-bridge dc–ac converter without an external dc source, is connected between the two converters. The voltage compensator generates an ac voltage that counteracts the ripple voltage on the output of the boost converter. Thus, the input of the grid-tie inverter is a dc voltage equal to the average value of the voltage *v*dc across the dc-link capacitor *C*dc. ac component of *v*dc. At the same time, the stable dc level of *va* can be obtained by.

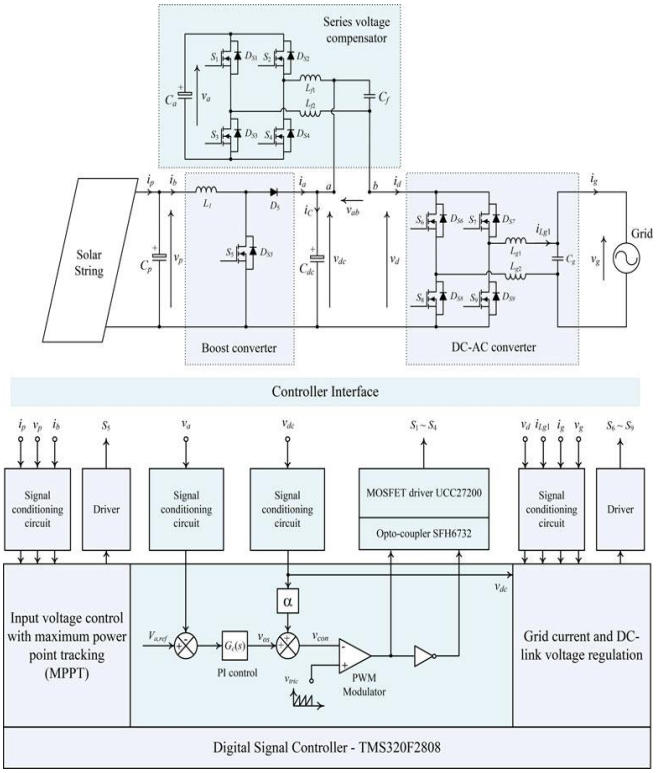

Voltage control, which guarantees the compensator just handles the responsive power in the relentless state. Amid the relentless state operation, vcon squares with the molded air conditioning segment of αvdc. It is then used to contrast and the triangular carrier waveform in the pulse width modulation modulator to generate the voltage vab having a similar phase and amplitude with Δvdc. Without any outer power supply, the power dispersal of the voltage compensator is acquired from the dc interface. For all intents and purposes, rather than an unadulterated air conditioning voltage, both vab and vcon comprises of air conditioning segment, as well as little measure of the dc segment. Since the input current of the grid-tie inverter comprises of the dc part, some power will be consumed by the compensator if vab comprises of the dc segment. Deductions of the parameters in the control are shown.

III. SYSTEM CHARACTERISTICS

The grid voltage *vg* and the output grid current *ig* can be expressed as

$vg\ (t) = Vg \sin \omega t$ (1)

$ig\ (t) = Ig \sin(\omega t + \varphi)$ (2)

where *Vg* and *Ig* are the amplitude of *vg* and *ig* , respectively,

$\omega = 2\pi f$ is the angular line frequency, *f* is the line frequency,

and φ is the phase difference between *vg* and *ig* .

Based on (1) and (2), the instantaneous output power *pg* is

$pg\ (t) = vg\ (t) ig\ (t)$

$= 2Pg \cos \varphi \sin \omega t \sin(\omega t + \varphi)$ (3)

where $Pg = Vg\ Ig\ 2 \cos \varphi$ is the average output power.

By applying the Kirchhoff's current law at the node of the dc-link capacitor *C*dc, the relationship among the output current *ia* of the boost converter, the dc-link capacitor current *iC* , and input current *id* of the inverter can be expressed as

$iC\ (t) = ia\ (t) - id\ (t)$. (4)

The dominant component of Δ*v*dc is the double of the line frequency harmonics. For the sake of simplicity in the analysis, Δ*v*dc is expressed as

$\Delta vdc(t) = |\Delta V dc| \sin(2\omega t + \theta)$ (5)

where $|\Delta V dc|$ is the magnitude of Δ*v*dc and θ is the phase angle of Δ*v*dc.

A. Steady-State Characteristics of the Voltage Compensator

Since the voltage compensator counteracts the ripple voltage on the dc-link capacitor only, the input voltage of the grid-tie dc–ac converter, *vd* , is equal to *V*dc. By using (3), the input current of the dc–ac converter, *id* , can be expressed as

$id\ (t) = pg\ (t)\ V dc$

$= Pg\ V dc \cos \varphi[\cos \varphi - \cos(2\omega t + \varphi)]$. (6)

By substituting (5) and (6) into (4),

$\gamma \cos(2\omega t + \theta - \delta)$

$= Pg\lambda V dc \cos \varphi \cos(2\omega t + \varphi)$ (7)

where $\gamma = \_PgV d\ c\_2+ (2\omega C dc V dc)2$,

$\delta = \tan{-}1\_Pg2\omega C d\ c\ V\ 2d\ c\_$,

and $\lambda = |\Delta V d\ c\ |V d\ c$ is the ripple factor.

Detailed proof of (7) is given in the Appendix.

By equating the magnitude and phase angle of the LHS and RHS of (7), the following equations can be concluded

$|\Delta V dc| = Pg\gamma \cos \varphi$(8a)

$\theta = \varphi + \delta$. (8b)

By substituting (8) into (5), the ripple voltage on the dc-link capacitor is

$\Delta vdc(t) = Pg\gamma \cos \varphi \sin(2\omega t + \varphi + \delta)$

$= \lambda V dc \sin(2\omega t + \varphi + \delta)$. (9)

According to (9), the relationship among the dc-link capacitance *C*dc, output phase angle φ, and the ripple factor λ is

$Cdc = Sg2\omega V\ 2dc\_1\lambda 2- \cos 2\ \varphi$ (10)

where *Sg* is the apparent power of the solar inverter.

Detailed proof of (10) is given in the Appendix.
Thus, for a given apparent power *Sg* , the required value of *C*dc will increase as the power factor cos *φ* decreases. Thus, one of the design constraints is based on considering the minimum power factor. For example, as stated in the statutory requirement

VDE-AR-N 4105, the minimum power factor is 0.9.
As the compensator handles ripple voltage only (i.e., *vab* = Δ*v*dc), the ratio between the apparent power handled by the compensator, *Sab* , and the apparent power of the whole system is

Sab Sg= *vab,*rms *id,*rms *vd,*rms *id,*rms
=/Δ*V*dc/√2*V*dc (11).

where *vab,*rms and *vd,*rms are the rms values of *vab* and *vd*, respectively, and *id,*rms is the rms value of the input current of the dc–ac converter.

Thus, as Δ*V*dc _ *V*dc, the power rating of the compensator is much smaller than that of the whole system. The voltage across the capacitor *Ca* , *va* , is regulated at *Va,*ref by using the control mechanism depicted in Fig. 1. If *va*<*Va,*ref , energy will be absorbed from the dc link, and vice versa. When *va*=*Va,*ref , the voltage compensator will ideally absorb zero power. Based on (6) and (9), the average power absorbed by the voltage compensator *Pab* is

Pab =1*T*_*T*0*vab* (*t*)*id* (*t*)*dt*
= −*P*2*g* sin *δ*2*γV*dc cos2*φ* (12)
where the period *T* = *π* / *ω*.

Thus, based on (12), if the compensator only generates the ripple voltage on the dc-link capacitor, it will generate active power. In order to maintain the power balance for stabilizing *va* at *Va,*ref , a small voltage offset at *vab* , *Vab* ,
appears *Vab* =−*PabId*
= *Pg* sin *δ*2*γ* cos2 *φ*. (13)

The relationship between *vab* and *va* can be expressed as
vab (*t*) = *v*con(*t*) *V*tric *va* (*t*)
= *α*v*dc(*t*) + *v*os(*t*)*V*tric*va* (*t*)
= *αPgγV*tric cos *φ* sin(2*ωt* + *φ* + *δ*) *va* (*t*)+
*αV*dc + *v*os(*t*)*V*tric*va* (*t*). (14)
The first term *αPg* sin(2*ωt*+*φ*+*δ*)
*γV*t r ic cos *φ* *va* (*t*) represents the ripple voltage compensation on the dc-link capacitor. The second term*αV*d c+*v*o s (*t*) *V*t r ic *va* (*t*) represents the dc component, related to the power balance described in (13). Thus, asymmetrical PWM switching occurs.

Fig. 2(a) and (b) present the operating modes of the compensator using a full bridge. When *S*2 and *S*3 are on, the capacitor *Ca* is charged by the load current *id* . Conversely, when *S*1 and *S*4 are on, the capacitor *Ca* is discharged by *id*. Fig. 2(c) shows the waveforms of the dc-link capacitor voltage *v*dc, modulating signal *vm*, triangular carrier signal *v*tric , and the voltage across *Ca* , *va* . The dc component on *vab* is very small. It is observed to be 2.1 V, about 0.5% of the average dc-link voltage of 400 V in the 2-kW inverter system, which will be described in Section V. Thus, such dc component is neglected in the following discussion.

IV. MATLAB/SIMULATION RESULTS

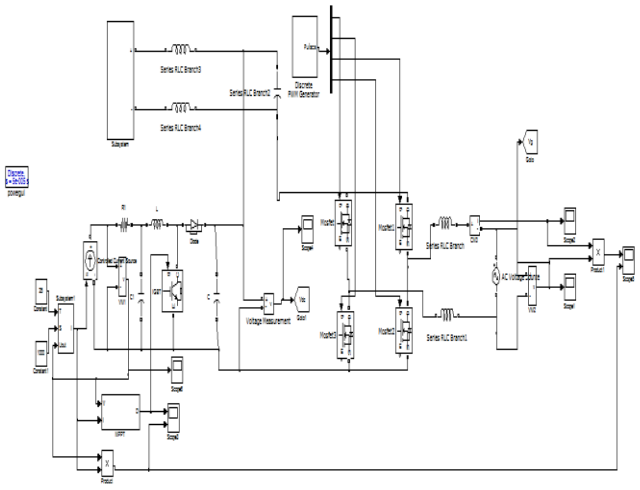

Fig 1:Grid-tie solar inverter with a series voltage compensetor.

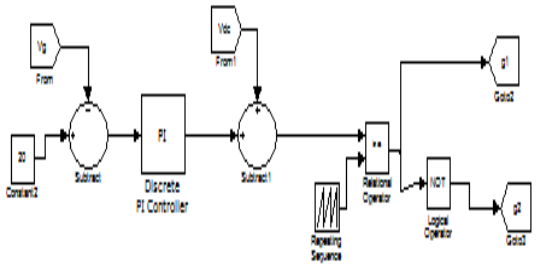

Fig 2:Control scheme

The dc-link voltage *v*dc and the input voltage of the voltage compensator *va* are sensed. The scaling factor *α* is the ratio between *V*tric and *Va,*ref , where *V*tric is the amplitude of the triangular carrier signal *v*tric in the PWM controller and *Va,*ref is the voltage reference for the input voltage of the voltage compensator. The difference between *Va,*ref and *va* is processed by a PI controller *G*(*s*) to give an offset voltage *v*os . The control signal *v*con is obtained by combining *α* *v*dc with *v*os. The dc component of *α* *v*dc is ideally cancelled in *v*con by *v*os as *V*os =−*αV*dc, where *V*os and *V*dcare the dc component of *v*os and *v*dc, respectively. With such arrangement, it is unnecessary to use a high-pass filter to extract the

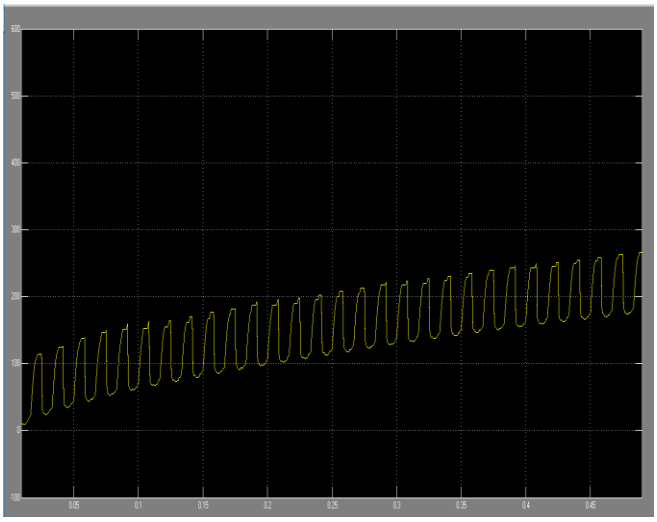

Fig 3:Voltage across DC-Link capacitance

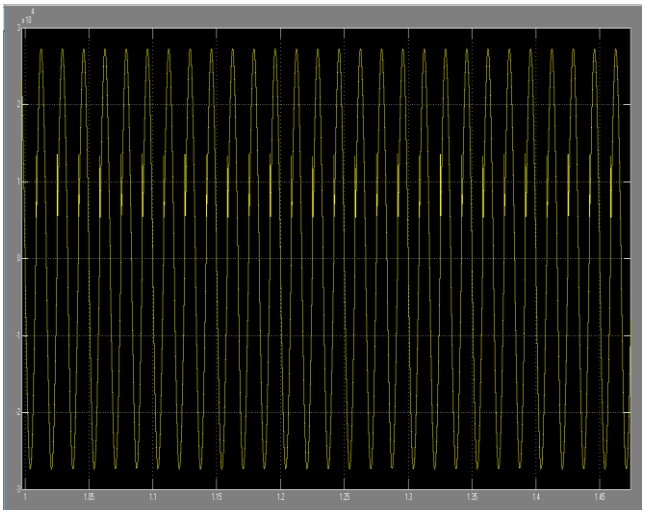

Fig 4:current across series voltage compensator

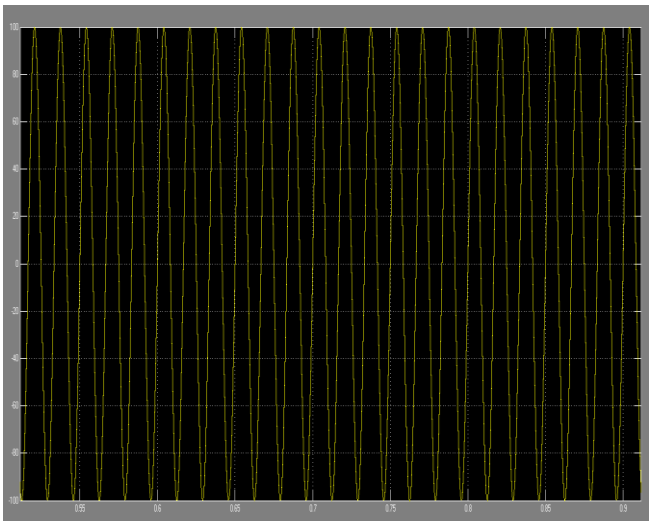

Fig 5 voltage across series voltage compensator

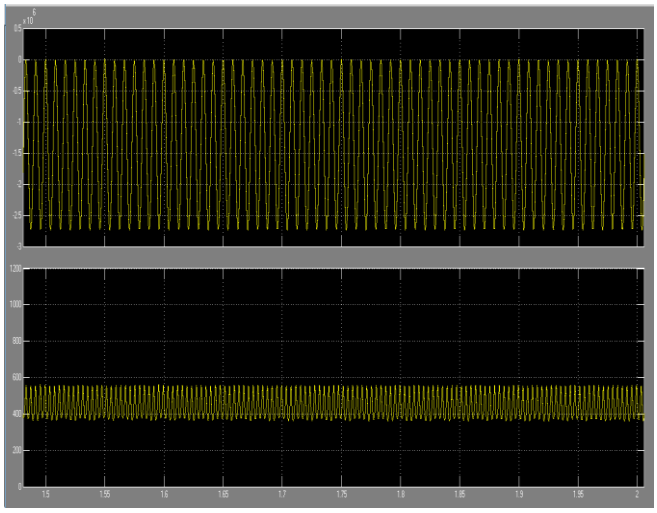

Fig 6: o/p power across Grid -Tie solar inverter

CONCLUSION

This paper report broadens the investigation of the idea proposed in which an arrangement voltage compensator is utilized to diminish the dc-connect capacitance. Such idea is connected to a grid-tie solar inverter. The modeling and plan of the arrangement voltage compensator has been introduced. Contrasted with this project report have the accompanying unmistakable exchanges:

1) The unfaltering state power oversaw by the arrangement voltage compensator is generally steady in the ac– dc– dc system, while the solar inverter has to process time-differing air conditioning power. Thus, connections among the front-organize boost converter, compensator, and output dc– air conditioning converter, have been talked about.

2) Reference gives the static characteristics of the arrangement voltage compensator just, while this project report gives both static and dynamic characteristics of the whole system.

3) The outside characteristics of the whole system have been given.

4) A definite examination on the execution expenses of the electrolytic capacitors and arrangement voltage compensator has been given.

A 2 kW, 220-V, 50-Hz model inverter has been worked to contrast the results and the electrolytic capacitors and with the compensator, separately. The experimental results show that, with the compensator, a 90% reduction of dc-interface capacitance and more than eight times augmentation of evaluated lifetime can be achieved. The frequency reaction of the whole system is additionally confirmed by explore. The execution cost of

the compensator is similar to that of electrolytic capacitors for 400-V applications. For 800-V applications, the usage cost of the compensator is lower than that of the electrolytic capacitors. The fundamental reason is that multiple arrangement associated electrolytic capacitors are required for high-voltage applications, while film capacitors of high-voltage rating are accessible.

REFERENCES

[1] A. Braham, A. Lahyani, P. Venet, and N. Rejeb, "Recent developments in fault detection and power loss estimation of electrolytic capacitors," IEEE Trans. Power Electron, vol. 25, no. 1, pp. 33–43, Jan. 2010.

[2] N.Blattau andC.Hillman, "Has the electronics industrymissed the boat on Pb-free?–failures in ceramic capacitors with Pb-free solder interconnects," in Proc. 5th Int. Lead Free Conf. Electron. Components Assemblies, San Jose, CA, USA, Mar. 18–19, 2004.

[3] G. Terzulli, Film Technology to Replace Electrolytic Technology in Wind Power Applications, AVX Technical Note, 2010.

[4] Film Capacitors for Industrial Applications, EPCOS Application Note, EPCOS AG, Munich, Germany, 2007.

[5] S. Harb and R. S. Balog, "Reliability of candidate photovoltaic module integrated- inverter (PV-MII) topologies—a usage model approach," IEEE Trans. Power Electron., vol. 28, no. 6, pp. 3019–3026, Jun. 2013.

[6] P. Pelletier, J. M. Guichon, J. L. Schanen, and D. Frey, "Optimization of a DC capacitor tank," IEEE Trans. Ind. Appl., vol. 45, no. 2, pp. 880–886, Mar./Apr. 2009.

[7] D. Lamar, J. Sebastian, M. Arias, and A. Fernandez, "On the limit of the output capacitor reduction in power-factor correctors by distorting the line input current," IEEE Trans. Power Electron., vol. 27, no. 3, pp. 1168–1176, Mar. 2012.

[8] I. S. Freitas, C. B. Jacobina, and E. C. Santos Jr., "Single-phase to singlephase full-bridge converter operating with reduced AC power in the DClink capacitor," IEEE Trans. Power Electron., vol. 25, no. 2, pp. 272–279, Feb. 2010.

[9] B.G.Gu and K. Nam, "A DC-link capacitor minimization method through direct capacitor current control," IEEE Trans. Ind. Appl., vol. 42, no. 2, pp. 573–581, Mar./Apr. 2006.

[10] H. Song, D. Oh, K. Nam, and S. Kim, "Method for controlling voltage of DC-link for electric vehicle," U.S. Patent 7 528 566, May 5, 2009.

[11] J. Ying, Q. Zhang, A. Qiu, T. Liu, X. Guo, and J. Zeng, "DC-DC converter circuits and method for reducing DC-bus capacitor current," U.S. Patent 7 009 852, Mar. 7, 2006.

[12] R. X. Wang, F. Wang, D. Boroyevich, R. Burgos, R. X. Lai, P. Q. Ning, and K. Rajashekara, "A high power density single-phase PWM rectifier with active ripple energy storage," IEEE Trans. Power Electron., vol. 26, no. 5, pp. 1430–1443, May 2011.

[13] H. B. Li, K. Zhang, and H. Zhao, "Active DC-link power filter for single phase PWM rectifiers," in Proc. IEEE Int. Conf. Power Electron. Asia, 2011, pp. 2920–2926.

[14] X. Du, L. W. Zhou, H. Lu, and L. M. Tai, "DC link active power filter for three-phase diode rectifier," IEEE Trans. Ind. Electron., vol. 59, no. 3, pp. 1430–1442, Mar. 2012.

[15] P. Krein, R. Balog, and M. Mirjafari, "Minimum energy and capacitance requirements for single-phase inverters and rectifiers using a ripple port," IEEE Trans. Power Electron., vol. 27, no. 11, pp. 4690–4698, Nov. 2012.